

2010

Cooling of a Reciprocating Compressor through Oil Atomization in the Cylinder

Rodrigo Kremer

Embraco

Jader R. Barbosa

Federal University of Santa Catarina

Cesar J. Deschamps

Federal University of Santa Catarina

Follow this and additional works at: <http://docs.lib.purdue.edu/icec>

Kremer, Rodrigo; Barbosa, Jader R.; and Deschamps, Cesar J., "Cooling of a Reciprocating Compressor through Oil Atomization in the Cylinder" (2010). *International Compressor Engineering Conference*. Paper 1986.
<http://docs.lib.purdue.edu/icec/1986>

This document has been made available through Purdue e-Pubs, a service of the Purdue University Libraries. Please contact epubs@purdue.edu for additional information.

Complete proceedings may be acquired in print and on CD-ROM directly from the Ray W. Herrick Laboratories at <https://engineering.purdue.edu/Herrick/Events/orderlit.html>

Cooling of a Reciprocating Compressor through Oil Atomization in the Cylinder

Rodrigo KREMER^{1,2}, Jader R. BARBOSA Jr.*¹, Cesar J. DESCHAMPS¹

¹POLO – Research Laboratories for Emerging Technologies in Cooling and Thermophysics
Federal University of Santa Catarina, Department of Mechanical Engineering
Florianopolis, SC, 88040-900, Brazil

²Embraco Compressors
Joinville, SC, 89219-901, Brazil

* Corresponding Author (Phone/Fax: +55 48 32345166, E-mail: jrb@polo.ufsc.br)

ABSTRACT

We present an experimental analysis of the influence of atomization of lubricant oil in the cylinder of a reciprocating refrigeration compressor. During compression, oil atomization enhances heat removal from the refrigerant gas, which results in a temperature decrease of the compressor components. A prototype was constructed and tested with R-134a in a fully instrumented gas-cycle calorimeter. Experimental results are presented for the temperature distribution in the compressor components. The results are further explored in the light of a calculation methodology based on macroscopic control volume formulations of the mass and energy conservation principles for the compression chamber coupled with an overall compressor energy balance.

1. INTRODUCTION

A thorough understanding of the energy transformations taking place inside compressors is necessary for improving their efficiency and of the refrigeration systems of which they are an essential part. Broadly speaking, the energy losses in a compressor are divided into (i) electrical, (ii) mechanical, (iii) thermodynamic and (iv) cycle losses (Possamai and Todescat, 2004). Thermodynamic losses involve the refrigerant flow inside the compressor. These are mostly associated with valve flows (viscous friction and flow reversal), gas leakage through the piston-cylinder gap and refrigerant superheating that occurs in the suction process and during vapor compression. According to Ribas (2007), for an R-134a household refrigeration compressor at the ASHRAE LBP condition, around 50% of the thermodynamic losses are due to suction gas superheating. This superheating causes a reduction of the volumetric efficiency and an increase of the compression work per unit mass (Gosney, 1982).

Many aspects of compressor cooling have been addressed in the past. Dutta *et al.* (2001) investigated theoretically and experimentally the effect of liquid refrigerant injection in scroll compressors using R-22. A decrease in the vapor temperature during compression was observed. However, the extra work required to compress the vaporized refrigerant gave rise to a decrease in the compressor performance. The experimental and numerical studies of Coney *et al.* (2002) quantified the decrease in power consumption (approximately 28%) associated with the atomization of water in air reciprocating compressors. Ooi (2005) evaluated numerically the injection of liquid refrigerant in a rotary compressor, taking into account the influence of the nozzle diameter and its position in the compression chamber. He concluded that it is more advantageous to inject the liquid shortly before the discharge of the gas to benefit from the latent heat transfer without the penalty of compressing a volume of gas that is not used for generating cooling capacity. Bonjour and Bejan (2006) demonstrated the existence of an optimal configuration for the distribution of cooling water in a multi-stage ammonia compressor that minimizes the compressor power. Wang *et al.* (2007) investigated theoretically two performance improvements for reducing the compressor power for several refrigerants. The first option was to cool the motor by external means other than using the suction gas. The second was to combine the processes of isothermal and isentropic compression. Their analysis demonstrated that the first option is more advantageous for low back pressure (LBP) rather than high back pressure (HBP) applications for

all refrigerants investigated. The second option showed that the compression power can be reduced by up to about 16% depending on operating conditions and working fluid.

In previous work (Kremer *et al.*, 2007, 2008), we presented a heat transfer model for the atomization of oil droplets in the cylinder of R-134a and R-717 reciprocating compressors, respectively. Oil atomization promotes an increase in the heat transfer surface area which enhances heat removal from the vapor. The resulting cooling effect also contributes to lowering the overall thermal profile of the compressor parts and, consequently, the initial compression temperature. In quantitative terms, for R-134a, atomization of oil at 45°C with an average flow rate of 0.916 kg/h gave rise to a maximum temperature reduction of 25°C at the top dead center (TDC). The initial compression temperature decreased from 58.8 to 44.6°C, illustrating the large potential for reducing losses due to refrigerant superheating.

In this paper, we report on experimental results of the cooling effect of oil atomization in the cylinder of a reciprocating compressor. A prototype was constructed and tested with R-134a in a fully instrumented gas-cycle calorimeter. Experimental results demonstrate a significant reduction of the temperature levels in the compressor components in comparison with the baseline condition. Parameters such as the cooling capacity, the compressor power and the COP are compared with the corresponding values predicted by the numerical model.

2. MATERIALS AND METHODS

2.1 Compressor Preparation

The compressor prototype shown in Fig. 1 has a split crankcase sealed with flat face bolt flanges and a silicone rubber gasket. A commercial hollow-cone nozzle (Lechler 212.004) was mounted flush on the wall of the compression chamber. Due to the nozzle and housing dimensions and space restrictions, the distance between the nozzle orifice and the valve plate is approximately 13 mm (see Fig. 1.c). The nozzle is fed by a pressurized 2-mm I.D. oil line which is connected to the oil separator of the calorimeter loop (see Section 2.2).

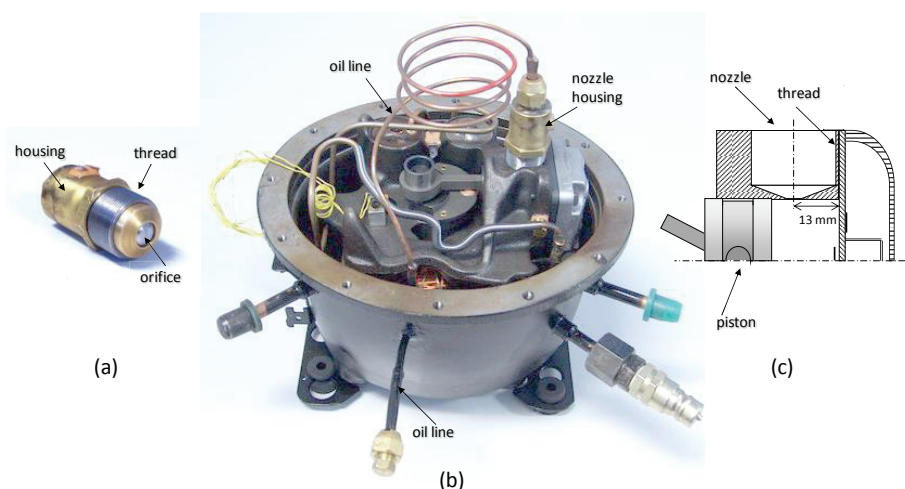


Figure 1: Compressor equipped with an oil nozzle. (a) Nozzle and threaded housing. (b) Compressor components and pressurized oil line. (c) Position of the orifice in the cylinder.

The temperatures of the compressor components were measured with 13 T-type thermocouples, as illustrated in Fig. 2. The temperature at which the oil enters the cylinder is assumed equal to that of the nozzle housing. The temperature of the gas entering the compression chamber is assumed equal to that measured at the suction chamber. Due to space restrictions, the temperatures of the cylinder wall and of the main bearing are measured by inserting the thermocouples into holes drilled in the compressor block so that the tip of the sensor is located at approximately 1mm of the surfaces of the cylinder and bearing, respectively. Although the uncertainty reported by the thermocouple manufacturer is $\pm 0.2^\circ\text{C}$, the one assumed in this study is $\pm 1^\circ\text{C}$ due to errors originating from the positioning and attachment of the thermocouples to the surfaces. The instantaneous gas pressure in the cylinder was

measured with a Kistler 601A absolute pressure transducer with a sampling frequency of 60kHz and an associated uncertainty of ± 0.12 bar.

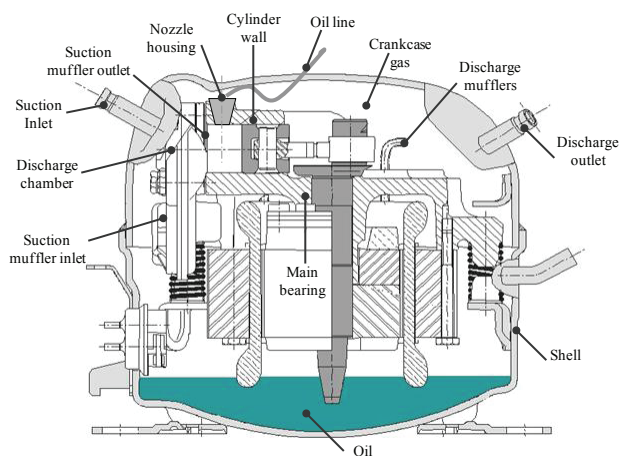


Figure 2: Compressor internal components and points of temperature measurement.

The influence of the split crankcase, atomization nozzle and pressure and temperature sensors on the compressor performance has been evaluated by comparing the refrigerant mass flow rate of the modified compressor prototype, but without oil atomization, with that of a compressor without the modifications. A reduction of the order of 10% in the mass flow rate has been observed. However, this does not represent a source of error since the modified prototype (without oil atomization) is the baseline for quantifying the influence of oil atomization on the compressor temperature profile.

2.2 Superheated Gas Cycle Calorimeter

The compressor was tested with R-134a in a superheated gas cycle calorimeter described schematically in Fig. 3. The compressor discharge pressure was regulated via a hand-operated needle valve (DV). An oil separator was installed in the discharge line, and was kept at a temperature above the saturation temperature of the refrigerant at the discharge pressure by means of an electric heater wrapped around its external surface. Downstream of DV, at an intermediate pressure between suction and discharge, an accumulator was installed to dampen pressure oscillations. A Coriolis-effect meter (MicroMotion) is used to measure the mass flow rate and, downstream of it, another hand-regulated needle valve (SV) is operated to expand the gas from the intermediate pressure down to the desired suction line pressure. The experimental error associated with the mass flow measurement is $\pm 0.15\%$, according to the manufacturer. A fixed inlet temperature of 32°C is set by an electric heater. The suction and discharge pressures are measured with HBM P3MB absolute pressure transducers (10 and 50 bar full-scale for the suction and discharge pressures, respectively) and the temperatures are measured with T-type thermocouples. The experimental uncertainty of the suction and discharge pressure measurements were estimated at ± 0.004 bar and ± 0.1 bar, respectively. The compressor power consumption was measured with a Yokogawa WT210 electric power transducer with an estimated error of $\pm 3\%$. After being separated from the discharge gas, the oil is driven through the oil line via a thermostatic bath for temperature control before being re-injected into the compressor, if valve OV is open. The experimental apparatus is fully integrated with a signal conditioning and data acquisition module.

2.3 Experimental Procedure

The experiments were performed with R-134a at evaporating and condensing pressures corresponding to -27°C and 42°C . The room temperature was maintained at 25°C . Tests were carried out with and without oil atomization and, in the latter, the oil injection temperatures was 45°C . The experimental procedure is as follows. Refrigerant is charged into the calorimeter under vacuum of 0.04 mbar needed to remove moisture and dissolved gases from the oil. Up to 6 hours are needed for steady-state and, in this period, the needle valves DV and SV are constantly adjusted to maintain the discharge and suction pressures to within $\pm 1\%$ of the specified condensing and evaporating pressures. In the tests with oil atomization, the temperature of the thermostatic bath is also continuously adjusted so as to keep the oil atomization temperature within the specified boundaries. The oil flow rate was not measured directly during the experiments. However, based on numerical analyses of the nozzle flow via CFD (Kremer, 2006) and

independent tests carried out outside the compressor with a constant nozzle pressure drop, with an oil injection temperature of 60°C, the oil flow rate was estimated at approximately 1 ± 0.2 kg/h.

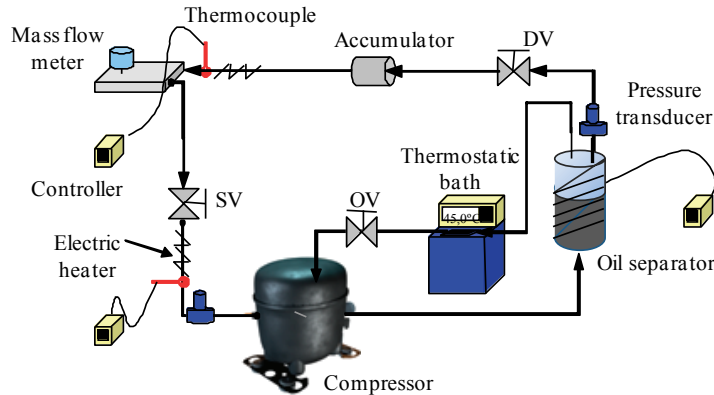


Figure 3: Schematic diagram of the superheated gas-cycle calorimeter.

The steady-state criterion establishes that, over an uninterrupted 45 min interval, the variation of the temperature readings should be less than 1°C and the variation of the measured compressor power and calculated cooling capacity (i.e., the product of the measured vapor mass flow rate and latent heat of vaporization at -27°C) should be less than 1%. When this condition is met, the temperature, mass flow rate and compressor power data are acquired and averaged for the next 10 min and the test is ended with the acquisition and averaging of 50 pressure-volume cycles.

An error propagation analysis (Kremer, 2006) yielded uncertainties of ± 4 and $\pm 5\%$ for the cooling capacity and coefficient of performance, respectively. At least five tests were carried out for each condition and the results reported in this paper consist of arithmetic averages of the data at each specific condition. Repeatability tests confirmed that the dispersion of the data with respect to the normal distribution was small, with deviations less than 3.5% of the average values.

3. MODELING

The mathematical model has been presented elsewhere (Kremer *et al.*, 2007; 2008), so only its main features will be discussed here. The control volume formulation of the vapor compression process consists of mass and energy balances given by (Ussyk, 1984),

$$\frac{dm}{dt} = \sum \dot{m} = \dot{m}_s - \dot{m}_d - \dot{m}_l - \dot{m}_{sr} + \dot{m}_{dr} \quad (1)$$

$$m \frac{du}{dt} = \dot{Q}_o + \dot{h}A_w(T_w - T) - p \frac{dV}{dt} - u \frac{dm}{dt} - (\dot{m}_d + \dot{m}_l + \dot{m}_{sr})h + \dot{m}_s h_{sc} + \dot{m}_{dr} h_{dc} \quad (2)$$

where the instantaneous cylinder volume is given by,

$$V = V_c - \frac{4\pi}{3} \sum_{m=0}^n N_{m,n} R_m^3 \quad (3)$$

$$\frac{dV}{dt} = \frac{dV_c}{dt} - \frac{4\pi}{3} \sum_{m=0}^n R_m^3 \frac{dN_{m,n}}{dt} \quad (4)$$

where V_c and its time differential are calculated from an algebraic relationship for the piston position as a function of the crankshaft angle (Ussyk, 1984). The compression cycle is divided into n time steps of size Δt and the droplets injected into the cylinder at a specified time-step (a so-called ‘family’) are assumed identical with respect to their size, velocity and temperature. In Eq. (4), $N_{m,n}$ is the number of droplets that were atomized into the cylinder at a

given instant m (the m^{th} family) and still are in the cylinder at an instant $n > m$. $N_{m,n}$ is computed via a population balance described in more detail by Kremer *et al.* (2007) and Kremer (2006).

Since the vapor pressure of the oil is small, it is assumed that only sensible heat transfer takes place between the droplets and the vapor. Temperature gradients inside the droplets and thermal interaction between droplets are ignored. Thus, the temperature of a droplet in group m at an instant n is calculated from,

$$\frac{dT_{m,n}}{dt} = \frac{3h_{m,n}}{\rho_o c_{p_o} R_m} (T - T_{m,n}) \quad (5)$$

where $h_{m,n}$ is the heat transfer coefficient between the gas and droplets calculated from the Ranz and Marshall (1952) correlation. The heat transfer rate between all oil droplets and the vapor is given by

$$\dot{Q}_o = 4\pi R_m^2 \sum_{m=0}^n N_{m,n} h_{m,n} (T_{m,n} - T) \quad (6)$$

The in-cylinder vapor compression and droplet heat transfer models were incorporated into an existing overall heat transfer model that integrates several compressor components (Fagotti *et al.*, 1994). Steady-state energy balance equations were written for each component and solved together with the transient in-cylinder vapor compression model. The suction and discharge processes were calculated via a one-degree-of-freedom model with natural frequency and damping coefficients specific for each valve. The resulting forces on the valves and their respective flow rates are obtained with effective force and effective flow areas derived from numerical simulations (Matos, 2002). In the oil atomization cases, the total flow rate through the discharge valve is calculated assuming a homogeneous two-phase density based on the discharge mass fraction of each phase (Kremer *et al.*, 2007). The reader is also referred to Kremer (2006) for a discussion on the numerical solution of the model equations.

4. RESULTS AND DISCUSSIONS

Table 1 shows the temperatures measurements at the positions indicated in Fig. 2 for the baseline (without oil atomization) and oil atomization conditions, respectively. As can be seen, a significant temperature decrease due to oil atomization at 45°C is observed, especially at the hottest spots such as the discharge chamber, discharge mufflers and cylinder wall. More importantly, this overall cooling effect is extended to the compressor parts associated with the suction gas superheating (suction inlet and suction muffler), which contributes to reducing the thermodynamic losses.

The P - V diagrams for the cases with and without oil atomization are presented in Fig. 4. The compression and expansion regions behave very similarly in both cases, with the main differences appearing in the suction and discharge processes, as can be seen from Figs. 5 and 6. Oil atomization increases the energy expenditure to take in and discharge the gas, which raises the compression power and hence the cycle mean effective pressure.

With oil atomization, the suction losses calculated based on the data of Fig. 5 increase by 17% with respect to the baseline. This increase can be attributed to a delay in the suction valve opening which gives rise to the more pronounced troughs in the pressure signal during the suction process. The delay itself can be caused by an increase in valve stiction (Khalifa and Liu, 1998) due to more oil between the valve and seat, or by changes in the pressure pulsation patterns in the suction muffler. By the same token, the discharge losses in the case with oil atomization increase by 57% with respect to the baseline (Fig. 6). The increase in the discharge pressure can be associated with (i) a larger flow restriction during discharge due to more oil between the piston and the valve plate, (ii) a larger mass of refrigerant being discharged due to the lower temperatures along the suction path, and (iii) stiction phenomena in the discharge valve.

Figure 7 shows the calculated valve displacement during discharge as a function of the crank angle for the baseline and atomization cases. The cylinder pressure is also shown for comparison purposes. As can be seen, in both cases, the discharge valve opens at 151.3 degrees from the bottom dead center (BDC). However, the pressure in the cylinder reaches the discharge value earlier for the oil atomization case. Thus, by comparing the pressures at which

the valve opens in both cases, one concludes that there is a delay of approximately 1 degree in the oil atomization case.

Table 1: Temperatures of the compressor components with oil atomization.

Components	Temperatures [°C]		Difference [°C]
	Baseline (no atomization)	Oil atomization	
Ambient (room) temperature	24.7	24.6	-0.1
Suction inlet	34.7	33.5	-1.2
Suction muffler inlet	45.6	41.7	-3.9
Suction muffler outlet	56.0	51.9	-4.1
Cylinder wall	89.7	66.1	-23.6
Discharge chamber	116.3	85.4	-30.9
Discharge mufflers	95.3	75.2	-20.1
Discharge outlet	76.7	67.8	-8.9
Crankcase gas	72.6	59.7	-12.9
Main bearing	79.1	62.5	-16.6
Shell	51.8	47.4	-4.4
Oil sump	60.1	55.6	-4.5
Oil line	44.1	36.2	-7.9
Nozzle housing	81.9	44.6	-37.3

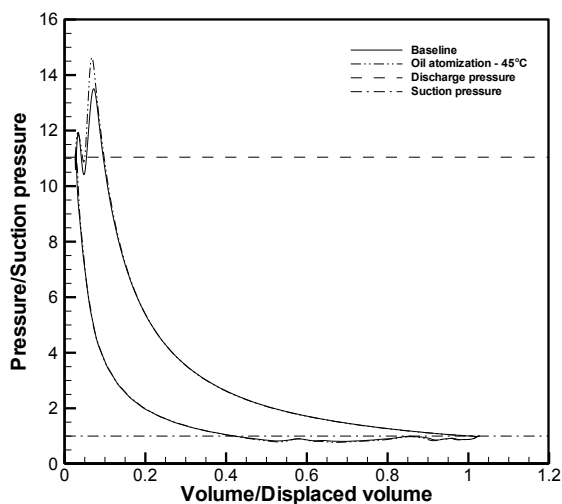


Figure 4: P - V diagram.

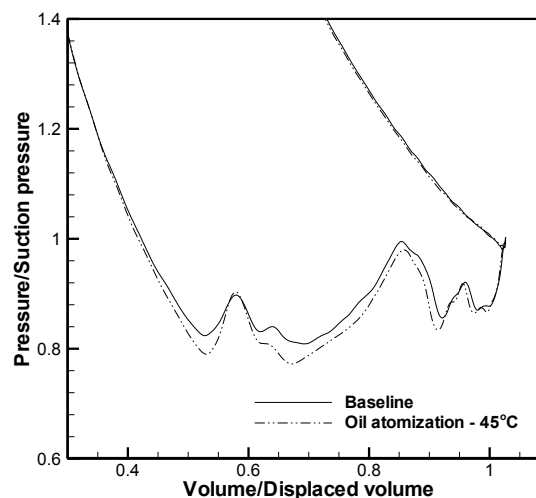


Figure 5: P - V behavior in the discharge region.

Figure 8 shows calculated heat transfer from the vapor as a function of the crank angle for atomization of oil at 45°C, with an average flow rate of 0.916 kg/h. The heat transfer during compression increases more sharply than the baseline and becomes positive earlier in the cycle showing a strong influence of droplet heat transfer. During expansion, heat transfer is similar in both cases (with and without oil) as a result of the very low velocity of the droplets remaining in the clearance volume after discharge. Figure 9 reveals a significant reduction of the vapor temperature (maximum of 25°C at the TDC) with oil atomization. The initial compression temperature decreases from 58.8 to 44.6°C, illustrating the large potential for reducing losses due to refrigerant superheating.

Table 2 compares the experimental and calculated cooling capacity, compressor power and coefficient of performance for the baseline and oil atomization cases. Although a satisfactory agreement is observed between model and experiments, the increase in the cooling capacity due to oil atomization in the cylinder is overshadowed

by the increase in the compressor power, which leads to a reduction in the COP. A number of phenomena can be associated with this unwanted increase in the compressor power, namely, the increase in the oil viscosity due to the compressor cooling, valve losses etc. All of these effects can be dealt with an improved design to make the cooling solution more attractive.

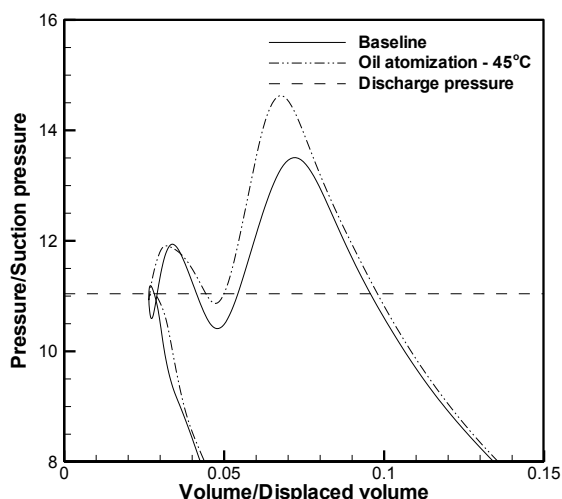
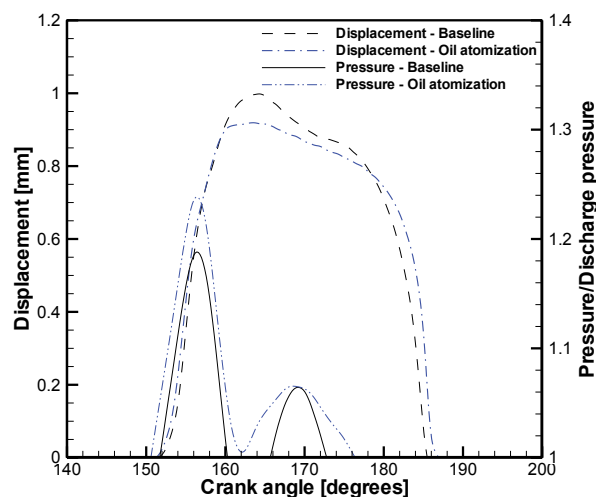
Figure 6: P - V behavior in the suction region.

Figure 7: Discharge valve displacement.

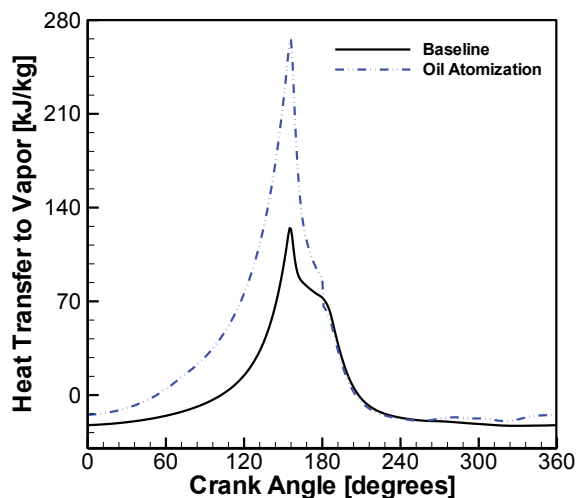


Figure 8: Heat transfer as a function of the crank angle.

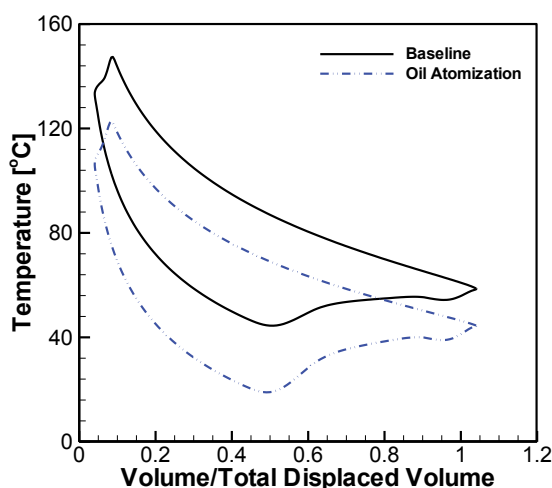
Figure 9: T - V diagram.

Table 2: Temperatures of the compressor components with oil atomization.

	Experimental			Calculated		
	\dot{Q}_e [W]	\dot{W}_c [W]	COP	\dot{Q}_e [W]	\dot{W}_c [W]	COP
Baseline	180.8	108.1	1.673	180.8	104.3	1.733
Atomization	183.0	118.4	1.546	183.6	113.1	1.623

5. CONCLUSIONS

In this paper, we presented an experimental analysis of the influence of atomization of lubricant oil in the cylinder of a reciprocating refrigeration compressor. The experimental results showed a significant decrease in the compressor thermal profile due to an enhanced heat removal from the refrigerant gas during compression. The results were in satisfactory agreement with a mathematical model but, although some increase in the cooling capacity was observed,

the coefficient of performance decreased as a result of higher compressor powers in the case with oil atomization. Design strategies could be sought to reduce the thermodynamic losses and make the cooling solution more efficient.

NOMENCLATURE

h	specific enthalpy (kJ/kg)	T	temperature ($^{\circ}\text{C}$)	l	Leakage
h	heat transfer coefficient ($\text{W}/\text{m}^2\text{K}$)	V	volume (m^3/s)	o	Oil
m	mass of vapor (kg)			r	reflux
M	mass of a single oil droplet (kg)	Subscripts		s	suction
\dot{m}	mass flow rate of vapor (kg/s)	c	cylinder	t	total
\dot{M}	mass flow rate of droplets (kg/s)	d	discharge	w	Wall

REFERENCES

- Bonjour, J., Bejan, A., 2006, Optimal Distribution of Cooling During Gas Compression, *Energy*, vol. 31, p. 409-424.
- Coney, M.W., Stephenson, P., Malmgren, A., Linnemann, C., Morgan, R.E., Richards, R.A., Huxley, R., Abdallah, H., 2002, Development of a Reciprocating Compressor Using Water Injection to Achieve Quasi-Isothermal Compression, *Proc. 16th Int. Compressor Engng. Conf. at Purdue*, CD-ROM.
- Dutta A.K., Yanagisawa, T., Fukuta, M., 2001, An Investigation of the Performance of a Scroll Compressor under Liquid Refrigerant Injection, *Int. J. Refrig.*, vol. 24, p. 577-87.
- Fagotti, F., Todescat, M.L., Ferreira, R.T.S., Prata, A.T., 1994, Heat Transfer Modeling in Reciprocating Compressors, *Proc. 12th Int. Compressor Engng. Conf. at Purdue*, pp. 605-610.
- Gosney, W.B., 1982, *Principles of Refrigeration*, Cambridge University Press.
- Khalifa, H. E, and Liu, X., 1998, Analysis of Stiction Effect on the Dynamic Compressor Suction Valve, *Proc. 14th Int. Compressor Engng. Conf. at Purdue*, p. 87-92.
- Kremer, R., 2006, *Theoretical and Experimental Analysis of the Influence of Oil Atomization in Compression Processes*, M.Eng. dissertation, Federal University of Santa Catarina (in Portuguese).
- Kremer, R., Barbosa Jr., J.R., Deschamps, C.J., 2007, Theoretical Analysis of the Effect of Oil Atomization in the Cylinder of a Reciprocating Compressor, *Proc. Int. Conf. on Compressors and their Systems*, London, paper C658-039.
- Kremer, R., Barbosa Jr., J.R., Deschamps, C.J., 2008, Theoretical Analysis of the Effect of Oil Atomization in the Cylinder of a Reciprocating Ammonia Compressor, *Proc. 19th Int. Compressor Engng. Conf. at Purdue*, Paper 1307.
- Matos, F.F.S., 2002, *Numerical Analysis of the Dynamic Behavior of Reed-Type Valves in Reciprocating Compressors*, D.Eng. thesis, Federal University of Santa Catarina (in Portuguese).
- Ooi, K.T., 2005, The Effects of Liquid Injection on the Performance of a Rotary Compressor”, *Proc. Int. Conf. on Compressors and their Systems*, London, p. 151-164.
- Possamai, F.C., Todescat, M.L., 2004, A Review of Household Compressor Energy Performance, *Proc. 17th Int. Compressor Engng. Conf. at Purdue*, CD-ROM.
- Ranz, W.E., Marshall, W.R., 1952, Evaporation from Drops – I and II, *Chem. Eng. Progr.*, vol. 48, p. 141 and 173.
- Ribas Jr., F.A., 2007, Thermal Analysis of Reciprocating Compressors, *Proc. Int. Conf. on Compressors and their Systems*, London, p. 277-287.
- Ussyk, M.S., 1984, *Numerical Simulation of Hermetic Reciprocating Compressors*, M.Sc. diss., Federal University of Santa Catarina (in Portuguese).
- Wang, X., Hwang, Y., Radermacher, R., 2008, Investigation of Potential Benefits of Compressor Cooling, *Appl. Thermal Eng.*, vol. 28, p. 1791-1797.

ACKNOWLEDGEMENTS

The material presented in this paper is a result of a long-standing technical-scientific partnership between the Federal University of Santa Catarina (UFSC) and Embraco. The authors are indebted to FINEP and CNPq through Grant No. 573581/2008-8 (National Institute of Science and Technology in Refrigeration and Thermophysics).